Science of the Total Environment 966 (2025) 178709

Contents lists available at ScienceDirect

Science of the Total Environment

journal homepage: www.elsevier.com/locate/scitotenv

Partitioning behavior and crystallization of urea, salts and water during stepwise dehydration of acidified human urine by evaporation

Ya Gao [*], Björn Vinnerås, Prithvi Simha [*]

Swedish University of Agricultural Sciences, Department of Energy and Technology, Box 7032, SE–750 07 Uppsala, Sweden

HIGHLIGHTS

- Maximum urine concentration factors of 30 at 20 °C and 43 at 70 °C by evaporation
- Water activity shown to be a reliable indicator of urine dehydration progress
- No nutrient loss during evaporation of sulfuric acid stabilized human urine
- Selective partitioning behaviors of nutrients for tailored fertilizer compositions

GRAPHICAL ABSTRACT

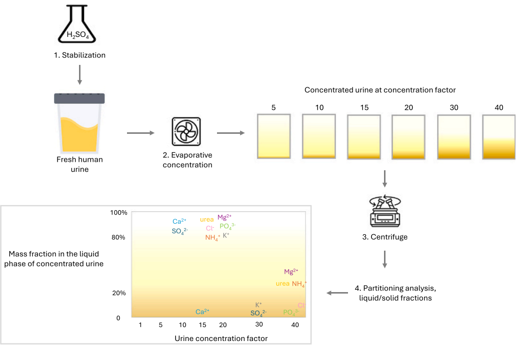

ARTICLE INFO

Editor: Huu Hao Ngo

Keywords:
Circular fertilizer
Decentralized sanitation
Eco-technology
Nutrient recycling
Resource recovery
Wastewater treatment

ABSTRACT

This study evaluated the stepwise evaporative concentration of acidified human urine, focusing on dehydration dynamics, crystallization sequence, and the partitioning of major constituents between liquid and solid phases. Unhydrolyzed urine, stabilized with sulfuric acid, was concentrated by convective evaporation, achieving concentration factors (CF) of up to 30 at 20 °C and 43 at 70 °C. Water activity (a_w) was a reliable indicator for monitoring urine dehydration progress, with a critical threshold of 0.3 a_w identified at CF 43, indicating tightly bound residual moisture which prevented further urine dehydration. No detectable losses of urea, major cations, or anions were observed throughout the treatment, suggesting that previous findings on nutrient loss were likely affected by analytical limitations as opposed to chemical degradation. Reconstitution to CF 1, followed by colorimetric analysis, was effective in determining nutrient content in viscous and solidified urine samples. At CFs above 30, over 80 % of urea, ammonium, and orthophosphate remained in the liquid phase, whereas sulphate, chloride, and potassium preferentially crystallized, forming compounds such as gypsum, syngenite, and biphosphammite. These findings demonstrate that adjusting dehydration conditions enables the nutrient profile of urine-derived fertilizers to be tailored to meet specific agricultural or environmental requirements. Overall, this study shows that stepwise evaporation-crystallization of acidified human urine can effectively produce multi-nutrient fertilizers with customizable nutrient compositions, thus enhancing targeted nutrient recirculation in agriculture.

---

[*] Corresponding authors.
E-mail addresses: ya.gao@slu.se (Y. Gao), Prithvi.Simha@slu.se (P. Simha).

https://doi.org/10.1016/j.scitotenv.2025.178709
Received 1 October 2024; Received in revised form 15 January 2025; Accepted 30 January 2025

1. Introduction

Interest in resource recovery from domestic wastewater has risen in recent decades, currently extending across multiple domains such as the recovery of nutrients, energy, water, and biosolids (Jain and Raghavan, 2024). Source-separating sanitation systems, which segregate domestic wastewater into distinct streams based on origin and composition, provide a fundamental basis for enhancing the efficiency of subsequent energy and resource recovery processes (Otterpohl et al., 2002). Source-separating sanitation systems vary based on the types of the wastewater streams they target. Domestic wastewater is typically divided into two major flows: black water (originating from the toilet and containing urine, faeces, toilet paper, and/or flush water) and grey water (derived from other household sources such as the bathroom and kitchen). Further separation of black water into nutrient-rich yellow water (urine) and brown water (faeces, toilet paper, and/or flush water) can be achieved using urinals or urine-diverting toilets. Urine diversion is especially efficient in nutrient recoveries because urine accounts for 80 % of nitrogen (N) and half of phosphorus (P) and potassium (K) in domestic wastewater but <1 % of the volume (Jönsson et al., 2005).

The concentrations of plant-available nutrients in urine are relatively low due to its high water content, which makes up 96 % of urine by mass (Vinnerås et al., 2006). This therefore presents logistical challenges for recycling urine as a liquid fertilizer, particularly for long-distance transport between urban nutrient recovery sites and agricultural lands (Trimmer and Guest, 2018). From the 1970s, research has sought to find alternatives to direct urine application, focusing on methods for extracting nutrients from urine for agricultural purposes (Harder et al., 2019). The methods researched throughout the early stage primarily focused on phosphorus recovery as struvite. However, since the mid-2000s, advancements in the field have resulted in the development of technologies that are capable of recovering a broad range of nutrients from urine (Aliahmad et al., 2022). A promising strategy involves concentrating urine by removing water and producing a solid fertilizer that captures all the nutrients, thereby simultaneously reducing logistical issues and maximizing nutrient recovery. For a comprehensive overview of the various urine concentration techniques, refer to the reviews by Maurer et al. (2006) and Martin et al. (2022).

Evaporation is considered the most straightforward method for removing water and reducing urine volume (Maurer et al., 2006). Within freshly excreted human urine, approximately 85 % of the nitrogen is present as urea (Kirchmann and Pettersson, 1995), which can be spontaneously hydrolyzed to ammonia, catalyzed by the enzyme urease (Mobley and Hausinger, 1989). Urease activity, which is widespread among microorganisms in soils and aquatic environments, plays an essential role in nitrogen metabolism (Mobley and Hausinger, 1989). A variety of microorganisms, including fungi, yeast, bacteria, and algae, can produce urease to utilize urea as their nitrogen source (Hasan, 2000), with bacteria being the most abundant ureolytic microorganisms in the environment (Udert et al., 2003). These bacteria are also commonly found in urinals, toilet bowls, and piping systems (Oki et al., 2010). The presence of urease is inevitable in urine collection systems and thus poses a challenge for water removal from urine by evaporation, because volatile ammonia produced by urea hydrolysis escapes into the atmosphere during evaporation (Hellström et al., 1999). One approach to mitigating nitrogen loss during evaporation is to stabilize nitrogen as non-volatile urea by inhibiting urease activity (Simha et al., 2020). Urease inhibition has been extensively studied, with various inhibitors demonstrating effectiveness. Heavy metal ions (Ag^{+}, Hg^{2+}, Cu^{2+}) inhibit urease by blocking the sulfhydryl groups at its catalytically active site (Shaw, 1954). Competitive inhibitors such as thiolate, phosphate, acetohydroxamic acids, and phenylphosphorodiamidate act by bridging the bi-nickel active sites within the urease metallocentre (Todd and Hausinger, 1989). Similar to other protein enzymes, the molecular structure of urease can be modified by adjusting the pH, which influences the charge state of ionic groups (Hasan, 2000). For human urine, urease activity can be reversibly inhibited by alkalization to increase the pH above 10.5 (Simha et al., 2022) or by acidification to decrease the pH below 3.0 (Hellström et al., 1999).

Previous research (Simha et al., 2023) has demonstrated the feasibility of producing bio-based solid fertilizer from source-separated human urine through a combination of acidification and evaporation, with all phosphorus and around 74 % of the nitrogen in urine recovered in the fertilizer product. However, the causes of nitrogen loss and the specific point at which nitrogen begins to volatilize during water removal remain unclear (Simha et al., 2023). In most urine dehydration systems, the water removal process is discontinued before complete dryness is achieved, necessitating the storage and transfer of partially dehydrated urine (Putnam, 1971). Thus, a more nuanced understanding of the kinetics of water removal from urine is required to optimize urine treatment processes. Water activity, which represents the unbound or 'free' water (Nielsen et al., 2012), could serve as an indicator for analyzing urine drying kinetics. By monitoring water activity, it may be possible to track the progress of water removal and determine the optimal endpoint, regarding minimized nitrogen loss while also ensuring manageable dehydration levels for storage and transport.

During the evaporation-crystallization process, dissolved organic and inorganic compounds in urine gradually precipitate as they reach their solubility limits (Jiang et al., 2017). Evaluating the stepwise crystallization of different constituents in urine during dehydration could be beneficial for optimizing the treatment of urine. For instance, crystal seeding is a critical step in large-scale crystallization processes because it significantly enhances nucleation and growth of crystals (Parambil and Heng, 2017). Indeed, knowledge of the crystallization sequence of salts in urine can inform targeted modifications, such as selective seed loading for specific crystals, tailored to the desired applications of urine-based products.

The changes that occur in the physical and chemical properties of acidified, unhydrolyzed urine during dehydration have yet to be systematically investigated. Therefore, this study aimed to analyze the partitioning behavior and crystallization of water, urea, and major cations and anions during the multistage evaporative concentration of acidified urine. A series of urine samples, stabilized with sulfuric acid and evaporated to different concentration factors (CFs), were characterized to evaluate these changes. The specific objectives were to: 1) determine the achievable maximum CF of acidified urine through convective evaporation at temperatures below 70 °C; 2) assess changes in water activity and unbound water content of acidified urine during evaporation; 3) evaluate the recovery of nitrogen in acidified urine during evaporation as a function of CF; 4) investigate behavior of urea, ammonium, orthophosphate, chloride, sulfate, potassium, calcium, and magnesium in acidified urine during evaporation; 5) analyze the partitioning of these constituents between the liquid and solid phases of urine relative to CF.

2. Methodology

2.1. Urine collection and acidification

Fresh human urine was anonymously donated by approximately 20 volunteers, comprised of both male and female donors aged between 25 and 65 years. Donations were provided individually in 500 mL sterile high-density polyethylene flasks at various times throughout the day. The collected urine was pooled, immediately dosed with 1.8 g sulfuric acid (≥95 %, VWR Chemicals) per liter of fresh urine to decrease the pH to below 3.0, and then thoroughly mixed. Over the course of one week, a total volume of 25 L was collected.

2.2. Concentrating acidified urine by evaporation

The concentration factor (CF) in this study was defined as the ratio of the initial mass of unconcentrated urine before evaporation to the final mass of concentrated urine after evaporation (Eq. 1).

$$\text{Concentration factor }(CF) = \frac{\text{Mass of unconcentrated urine before evaporation }(g)}{\text{Mass of concentrated urine after evaporation }(g)} \quad (1)$$

Acidified urine was concentrated by evaporation to achieve CFs of 5, 10, 15, 20, 30, 40, along with a maximum CF corresponding to the constant final mass under the specified evaporation conditions of the study. The CFs of 5, 10, 15, 20, and 30 were achieved by evaporating the urine at room temperature (20 ± 2 °C) with forced convective evaporation. The CF of 40 was reached by evaporating the urine at 50 °C, while the maximum CF was determined by evaporating the urine at 70 °C.

2.3. Sampling and analysis

Water activity of concentrated urine and unconcentrated urine (i.e., urine at CF 1) was measured using a water activity meter (AQUALAB TDL, METER Group, United States) with ± 0.005 a_w accuracy at 25 °*C. Prior* to the measurement, concentrated urine samples were thoroughly mixed to ensure homogeneity, and 1 g of urine from each CF was evenly spread across the bottom of an AQUALAB disposable sample cup (40106, METER Group, United States). The sample cup was then immediately loaded into the water activity meter and measurements were taken at 25 °C. The water activity values were recorded once the difference between three consecutive readings was <0.0005 a_w.

The total solids (TS) content of the acidified urine was considered equivalent to the final mass of the concentrated urine at the maximum CF, of which the constant weight was achieved at 70 °C. The remaining evaporable fraction, consisting of unbound water and volatiles, was calculated based on the TS content of the acidified urine.

The concentrated urine was centrifuged at 15,000 rpm at 20 °C for 5 min (Eppendorf, centrifuge 5424 R), to separate the liquid and solid phases. The mass of the separated liquid phase and the total mass of the concentrated urine were measured to determine the mass fraction of the liquid phase. Centrifugation and weighing were completed in duplicate for urine at each CF, and the average values of the mass fraction of the liquid phase were used for subsequent analysis.

The concentrations of urea, ammonia nitrogen (NH_3-N), orthophosphate phosphorus (PO_4^{3-}-P), potassium (K^+), chloride (Cl^-), sulfate (SO_4^{2-}), calcium (Ca^{2+}), and magnesium (Mg^{2+}) were analyzed using colorimetric methods with a Thermo Scientific™ Gallery™ discrete analyser. The concentrations of ammonia nitrogen (NH_3-N) were converted and reported as ammonium (NH_4^+) using its relative molecular mass. Similarly, orthophosphate phosphorus (PO_4^{3-}-P) concentrations were calculated and expressed as orthophosphate (PO_4^{3-}) for consistency in reporting nutrient concentrations under the acidic conditions used in this study. The analytical methods used for urea and each cation and anion are provided in Table S1 of the Supplementary Information (SI). Prior to these analyses, the liquid phase and the entire concentrated urine of each CF were reconstituted to CF 1 with Milli-Q water and filtered using a 0.45 μm syringe filter (Filtropur S, Sarstedt, Germany). To determine the total nitrogen concentration, concentrated urine was digested using a Spectroquant® Crack-Set 20 test kit (1.14963.0001), followed by an analysis for concentration of nitrate nitrogen. To determine the total phosphorus concentration, concentrated urine was digested using a Spectroquant® Crack-Set 10 test kit (1.14687.0001) and analyzed for concentration of orthophosphate. The concentrations of nitrate and orthophosphate were measured using the Thermo Scientific™ Gallery™ discrete analyser and the specific methods are outlined in Table S1 of the SI.

The concentration of an analyzed substance (urea or the above-mentioned ions) (S) in the liquid fraction of the concentrated urine ($C_{S,L}$ $[mg/g]$) was calculated using Eq. 2.

$$C_{S,L}\ [\mathrm{mg/g}] = \frac{\text{Mass of S in the liquid fraction [mg]}}{\text{Mass of the liquid fraction [g]}} \quad (2)$$

The concentration of S in the entire concentrated urine ($C_{S,Entire}$ $[mg/g]$) can be expressed as Eq. 3.

$$C_{S,\mathrm{Entire}}\ [\mathrm{mg/g}] = \frac{\text{Mass of S in the entire concentrated urine [mg]}}{\text{Mass of the entire concentrated urine [g]}} \quad (3)$$

The partitioning of S in the liquid phase of the concentrated urine, defined as the ratio of the mass of S in the liquid fraction to that in the entire concentrated urine, can be expressed as Eq. 4.

$$\text{Partitioning of S} = \frac{C_{S,L}}{C_{S,\mathrm{Entire}}} \times \frac{\text{Mass of liquid fraction [g]}}{\text{Mass of the entire concentrated urine [g]}} \quad (4)$$

3. Results

3.1. Concentrated urine and mass fraction of the liquid phase

The physical state of urine progressively changed during the evaporative concentration treatment (Fig. 1). The maximum concentration factor (CF) achieved was 43, corresponding to 97.7 % of reduction in urine mass, obtained by evaporation at 70 °C. Solid precipitation was observed in all the concentrated urine compared to the unconcentrated CF 1 urine. Clear separation between the liquid and solid phases was evident in urine at CFs of 5, 10, 15, 20, and 30 (Fig. S1 In the SI). At a CF >40, the concentrated urine exhibited a viscous texture with minimal residual moisture because >97 % of urine mass had been reduced.

The mass fraction of the liquid phase decreased as the urine was concentrated to higher CFs (Fig. 2). For concentrated urine at CFs below 30, the mass fraction of the liquid phase had a linear relationship with the urine CF. However, at CF 40, the liquid phase had a much lower mass fraction (0.24) which deviated from the linear regression model at lower CFs.

3.2. Water activity and remaining evaporable fraction

The TS content of urine was 23 g TS kg^{-1}, wherein 1.8 g TS kg^{-1} was attributed to the addition of sulfuric acid. The remaining evaporable fraction in the concentrated urine decreased linearly with increasing urine CF, which corresponded with the decrease in water activity (Fig. 3a). At the maximum CF of 43, all evaporable fraction of the acidified urine at 70 °C was assumed to be completely evaporated, resulting in a 98 % reduction in urine (Fig. 3b) and a decrease in water activity to the lowest observed value of 0.3 (Fig. 3a).

3.3. Fate of urea, cations and anions during evaporative concentration

There were no detected losses of urea or any cations or anions in the concentrated urine across all CFs. The relative concentrations of urea and the analyzed cations and anions in the reconstituted urine were consistent with those in the unconcentrated urine (Fig. 4). The slopes of the linear fits, which represents the relationship between the relative

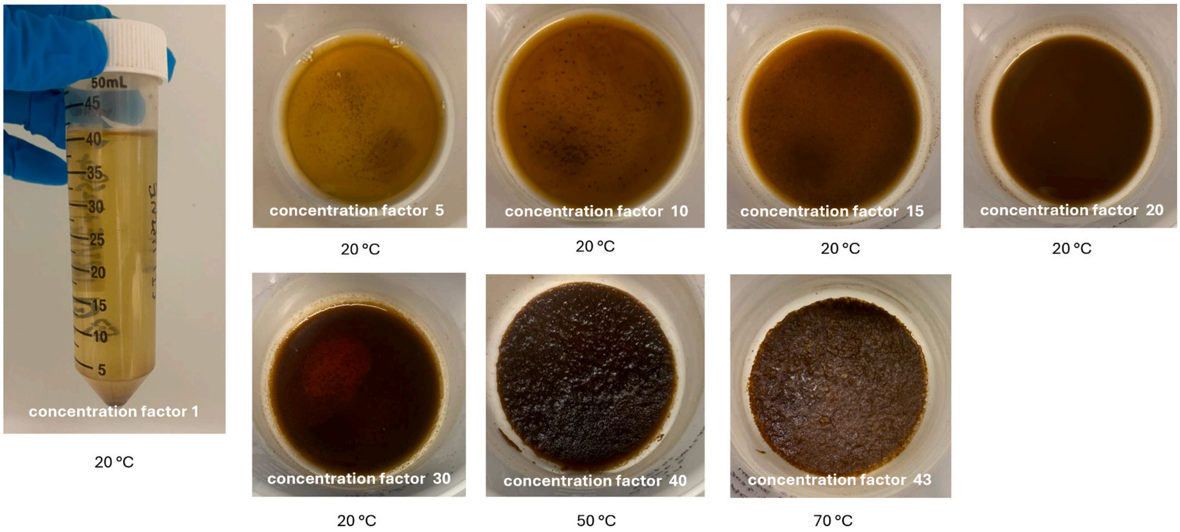

Fig. 1. Unconcentrated and concentrated urine at various concentration factors (CFs) of 5, 10, 15, 20, 30, 40, and 43, treated by sulfuric acid stabilization and stepwise evaporative concentration.

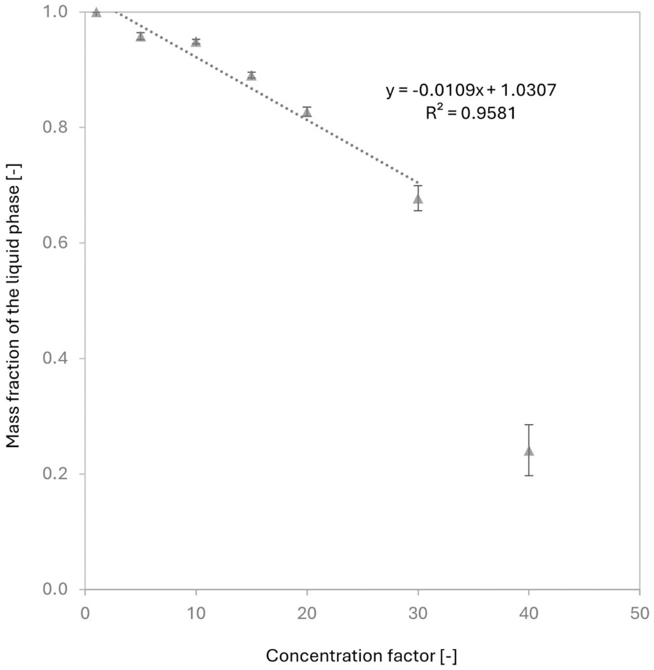

Fig. 2. The mass fraction of the liquid phase of urine at different concentration factors (CFs) of 1, 5, 10, 15, 20, 30, and 40. Urine was stabilized by sulfuric acid and concentrated by evaporation at 20 °C (CF <30) and 50 °C (CF 40), respectively. The values were averaged by two independent measurements. The linear regression was modeled excluding the data of the concentrated urine at CF 40.

concentration of the various constituents and the CF before reconstitution, were effectively zero, indicating minimal changes in the concentration of these constituents during evaporation (equations provided in Table S2 of the SI).

3.4. *Partitioning of urea, cations and anions in concentrated urine*

In urine concentrated to CF 30 (corresponding to a 96.7 % reduction in mass), >80 % of urea, ammonium, and orthophosphate remained in the liquid phase, whereas >95 % of sulfate, 34 % of chloride, and 72 % of potassium partitioned into the solid phase (Fig. 5). Urea (Fig. 5a), ammonium (Fig. 5b), and orthophosphate (Fig. 5c) began partitioning into the solid phase at CFs exceeding 20. Even at CF 40, 30 % of the urea and ammonium and 14 % of orthophosphate remained in the liquid phase. Potassium (Fig. 5d) and chloride (Fig. 5e) partitioned into the solid phase at CFs above 20, with only 7 % of the potassium and 16 % of the chloride remaining in the liquid phase at CF 40. Sulfate (Fig. 5f) began partitioning into the solid phase at CF 10, and by CF 40, <1 % of sulfate was retained in the liquid phase. Calcium (Fig. 5g) predominantly partitioned into the solid phase at CF 10. Magnesium (Fig. 5h) started to partition into the solid phase at CF 20, with 40 % retained in the liquid phase at CF 40.

4. Discussion

4.1. *Water activity as an indicator of urine dehydration progress*

Water exists in human urine in different forms, including ‘free’ or unbound water, as well as physically, chemically or biologically bound water. Water activity is defined as the ratio of the vapor pressure of water in an aqueous mixture to that of pure water at the same temperature (Blandamer et al., 2005). Pure water has a water activity of 1, while lower water activity values indicate a reduced content of unbound water. Measuring water activity of concentrated urine at different CFs provides insights into water behavior in the urine matrix during dehydration. When urine was concentrated to a CF below 20, corresponding to <95 % reduction in urine mass, the water activity remained above 0.75 (Fig. 3). This is consistent with the visual observations (Fig. 1), which showed minimal solid formation and >80 % of the mass in liquid form (Fig. 2). This suggests that at CFs below 20, most of the water remains unbound and can be readily removed through continued convective evaporation at 20 °C. Water activity dropped considerably to 0.6 (Fig. 3a) when urine was concentrated to CF 30, coinciding with significant precipitation of solids (Fig. 1). At this stage, only 30 % of the water remained unbound, while the rest likely became bound to organic metabolites and/or crystallized minerals within the solids through hydrogen bonds (Fig. 3a). Notably, CF 30 was the maximum level of urine dehydration achievable at 20 °C. In the hydrogen-bonded water structures, hydrogen bonds break and reform dynamically but the amount of bound water remains constant at a distinct temperature (Nielsen et al., 2012). This implies that an equilibrium among solids, unbound water, and bound water was established through the breaking and formation of hydrogen bonds in the concentrated urine matrix of CF 30 at 20 °C. However, increasing the evaporation temperature disrupted

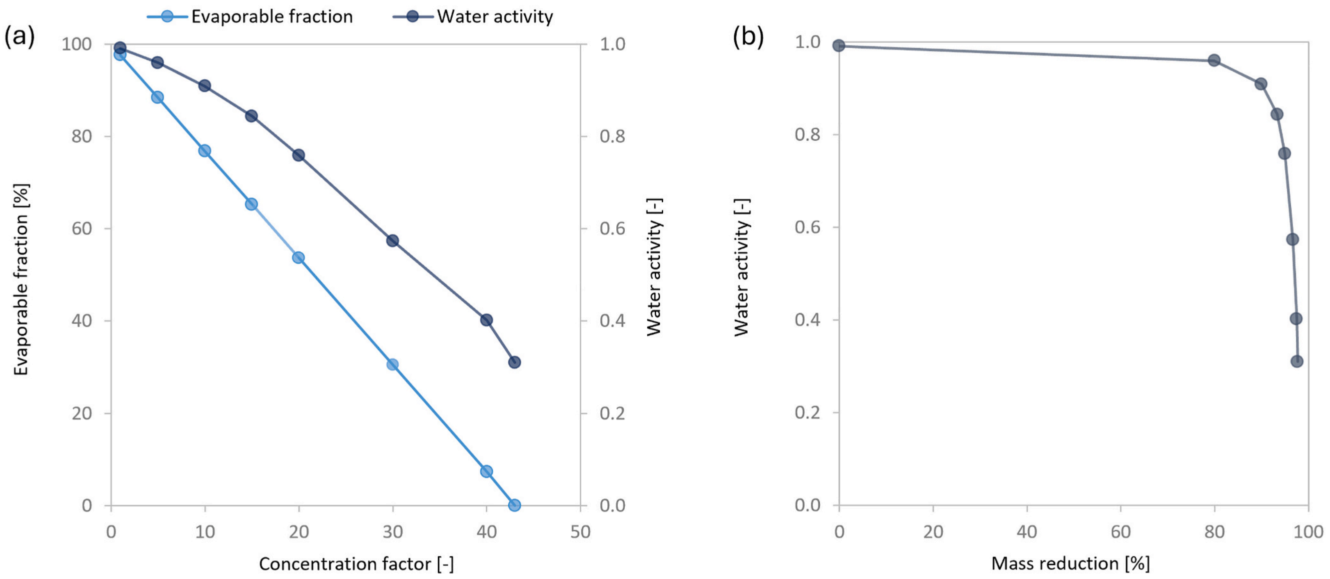

Fig. 3. Water activity and the remaining evaporable fraction of the concentrated urine versus urine concentration factor (CF) (a). Water activity versus mass reduction percentage of the concentrated urine (b). Urine was stabilized by sulfuric acid and concentrated by evaporation at 20 °C (CF < 30), 50 °C (CF 40) and 70 °C (CF 43), respectively.

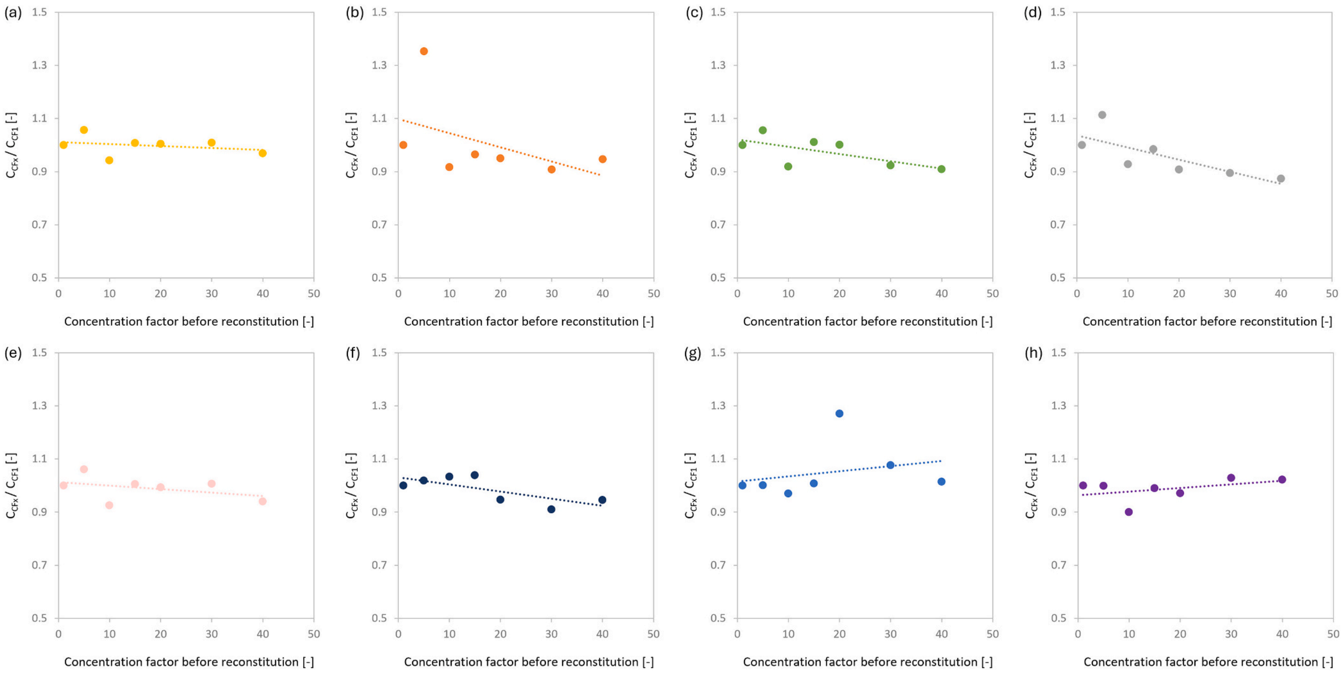

Fig. 4. Relative concentrations of urea (a), ammonium (b), orthophosphate (c), potassium (d), chloride(e), sulfate (f), calcium (g), and magnesium (h) in the reconstituted urine compared to the unconcentrated urine versus urine concentration factor (CF) before the reconstitution. Urine was stabilized by sulfuric acid and concentrated by evaporation at 20 °C (CF <30) and 50 °C (CF 40). Concentrated urine was reconstituted to CF 1 for urea and ion analyses. C_{CF1}: the concentration of urea/ion in the unconcentrated CF 1 urine; C_{CFX}: the concentration of urea/ion in the reconstituted (to CF 1) urine, of which the original CF is X. See Table S3 of the SI for mass balance calculations.

this equilibrium, allowing for further dehydration and enabling urine to reach higher CFs. The additional heat input facilitated the breakdown of hydrogen bonds, thereby promoting the evaporation of remaining unbound water.

A water activity of 0.3 was identified as a critical threshold for water removal from acidified urine by convective evaporation at 70 °C, indicating that most of the remaining water was tightly bound. Similar findings have been reported by Hostmark and Teigland (2009), who observed that the dewatering rate of low-viscosity peptone solutions through evaporation reduced by >90 % at a water activity of 0.3. The total solids (TS) content is typically determined by oven drying samples at 105 °C until constant weight. However, for samples with high contents of volatile organic compounds or certain inorganic salts, particularly those containing bicarbonates, a drying temperature at 70 °C is recommended to avoid losses of these compounds (Chowdhury et al., 2014; Peces et al., 2014). In the present study, concentrated urine at CF 43 was excluded from partitioning analysis because no liquid could be extracted after centrifugation at 15,000 rpm for 5 min (Fig. S2 of the SI).

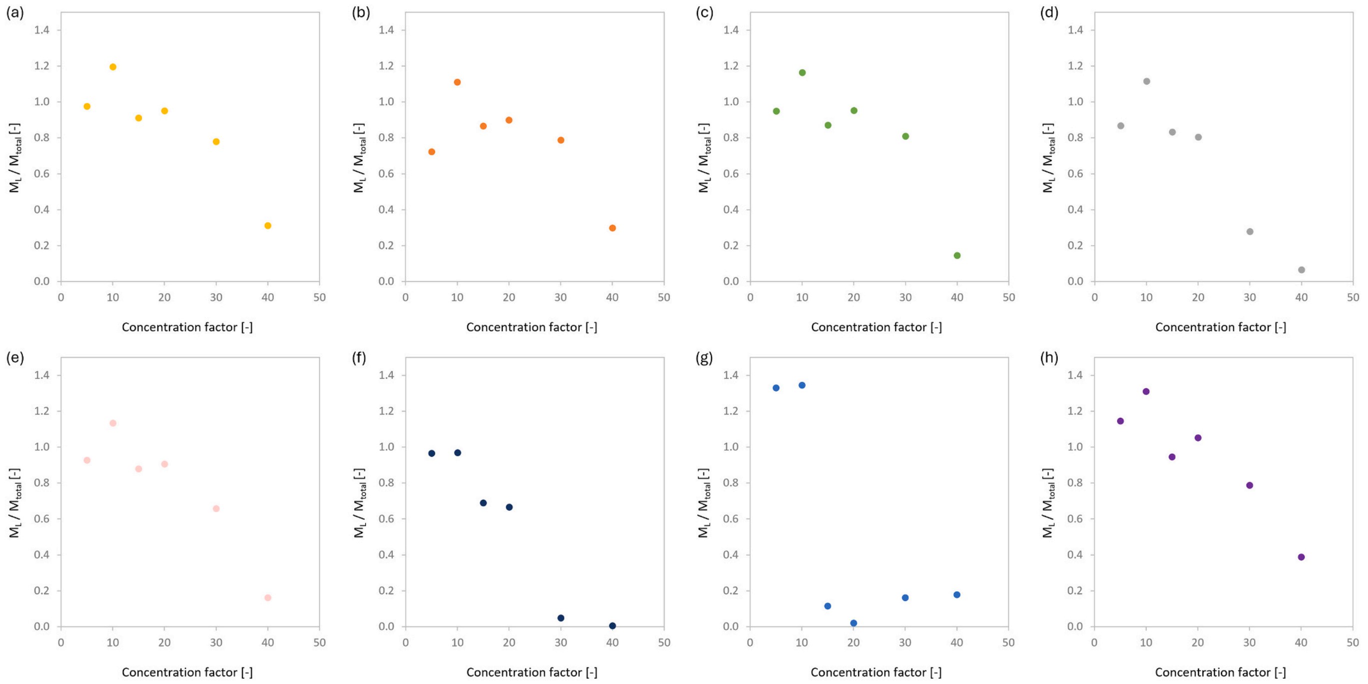

Fig. 5. Mass partitioning of urea (a), ammonium (b), orthophosphate (c), potassium (d), chloride(e), sulfate (f), calcium (g), and magnesium (h) in the liquid phase over the entire concentrated urine at different concentration factors (CFs). Urine was stabilized by sulfuric acid and concentrated by evaporation at 20 °C (CF <30) and 50 °C (CF 40). Concentrated urine was reconstituted to CF 1 for urea and ion analyses. M_L: the mass of urea/ion partitioned in the liquid phase of the concentrated urine. M_{total}: the total mass of urea/ion present in the concentrated urine.

This supports the assumption that the mass of urine concentrated to CF 43, which was dehydrated at 70 °C until constant weight, represents the TS content of acidified urine. Similar results have been noted by Getahun et al. (2020), who reported that a water activity of 0.3 corresponded to a moisture content of <10 % during the drying of fecal sludge. The remaining water in the sludge is proportionally higher in bound form, requiring significantly more energy input to remove the residual moisture (Getahun et al., 2020).

4.2. No loss of nutrients in acidified urine during evaporative concentration

No loss of urea was observed in the concentrated urine across all CFs (Fig. 4a), meaning it is unlikely that the nitrogen loss reported in a previous study (Simha et al., 2023) was a result of urea hydrolysis or the decomposition of cyanate derived from urea. Further, the total ammonia (Fig. 4b) and total nitrogen content (Fig. S3a in Supplementary Information) in concentrated urine remained consistent across all CFs, suggesting that the nitrogen loss noted in the previous study (Simha et al., 2023) may have resulted from analytical errors. The previous study used the Dumas dry combustion method for total nitrogen analysis of dehydrated urine. This method, although reliable, may be inappropriate when applied to fully dehydrated, acidified urine matrices, wherein incomplete combustion of organic nitrogen compounds or interference from residual acids could cause an underestimation of the nitrogen content. The consistent nitrogen content observed in this study, using an alternative analytical method, supports the conclusion that all nitrogen was retained in the urine treated by acidification and evaporative concentration. In this study, urea and ions were analyzed after reconstituting the concentrated urine. The consistency in the relative concentrations of urea, cation and anion across all urine CFs (Fig. 4) implies that no losses occurred during reconstitution. This implies that a straightforward compositional analysis can be conducted by reconstituting samples of concentrated acidified urine, thereby avoiding the challenges associated with analyzing viscous or solidified samples.

4.3. Implications for urine-derived fertilizer design

The partitioning behaviors of urea (Fig. 5a), ammonium (Fig. 5b), and orthophosphate (Fig. 5c) in concentrated urine were similar across different CFs, indicating that selective recovery for nitrogen or phosphorus alone in a stepwise dehydration-crystallization process would be challenging. Nevertheless, because nitrogen and phosphorus are both essential nutrients for plant growth, their simultaneous recovery in a multi-nutrient fertilizer is beneficial (Harder et al., 2019).

The extensive use of mineral fertilizer is a significant anthropogenic factor contributing to soil salinization (Litalien and Zeeb, 2020). It has been suggested that the salt content in urine-derived fertilizers could pose certain challenges in arid and semi-arid regions, particularly during dry seasons when limited water availability restricts the ability to fully wash out salts from soils (Medeiros et al., 2020). Higher evapotranspiration rates in these regions can lead to salt accumulation even during rainy seasons (Guizani et al., 2016). Considering this, the distinct partitioning behaviors of ions in urine offer opportunities for designing smart fertilizer formulations. For example, dehydrating urine to a CF around 30 and separating the solids before further dehydration could remove 95 % of sulfate and 34 % of chloride, while retaining all nitrogen and phosphorus. This would reduce the salt load during fertilizer application, making urine-based fertilizers more suitable for sensitive environments. In most cases, however, no significant soil salinization issues related to urine-based fertilizer application have been reported, except in arid or semi-arid areas (Martin et al., 2022).

4.4. Crystallization sequence during urine evaporation

Evaporation of complex aqueous matrices typically results in the sequential crystallization of simple salts, double salts, salt hydrates, and other more complex crystalline products (Voigt, 2001). During evaporation, the concentrations of ions in urine increased as water was removed. When the concentration of salt consisting of these ions exceeds the salt solubility limit, salt precipitation occurs along with evaporation

(Shokri-Kuehni et al., 2017). Thermodynamic modeling from a previous study (Simha et al., 2023) predicted that when >99 % of the water in acidified urine was removed (corresponding to the CF around 30), urea ($CO(NH_2)_2$), salammoniac (NH_4Cl), biphosphammite (KH_2PO_4), sylvite (KCl), syngenite ($K_2SO_4 \cdot CaSO_4 \cdot H_2O$), and görgeyite ($K_2SO_4 \cdot 5CaSO_4 \cdot H_2O$) would crystallize.

In this study, when acidified urine was dehydrated to a CF between 10 and 20, almost all of the calcium (Fig. 5g) and about 30 % of the sulfate (Fig. 5f) partitioned into the solid phase, suggesting the initial formation of calcium sulfate. Calcium sulfate occurs naturally in three different forms, which are each distinguished by their degree of hydration: gypsum ($CaSO_4 \cdot 2H_2O$), hemihydrate ($CaSO_4 \cdot 0.5H_2O$), and anhydrite ($CaSO_4$). The solubility of these forms is strongly influenced by solution temperature (Freyer and Voigt, 2003). At 25 °C, hemihydrate remains relatively soluble, and anhydrite does not crystalize in water at a measurable rate below 70 °C, with the transition temperature between gypsum and anhydrite around 55 °C (Freyer and Voigt, 2003). Hence, in concentrated urine at CF 10, calcium sulfate present in the solid phase is likely dominated by gypsum.

As urine was further dehydrated to a CF between 20 and 30, calcium concentration in the liquid phase became negligible (Fig. 5g), and potassium began to partition to the solid phase (Fig. 5d). Concurrently, there was a significant drop in sulfate concentration, which neared zero in the liquid phase (Fig. 5f). Assuming that gypsum forms between CF 10 and 20, the continuous removal of sulfate from the liquid phase at CFs above 20 suggests that the remaining sulfate, along with potassium in the liquid, and calcium sulfate in the solids, likely crystallized as syngenite ($K_2SO_4 \cdot CaSO_4 \cdot H_2O$) and görgeyite ($K_2SO_4 \cdot 5CaSO_4 \cdot H_2O$). This hypothesis aligns with a phase diagram of the $CaSO_4$ - K_2SO_4 - KNO_3 - $Ca(NO_3)_2$ - H_2O system developed by Jurisová et al. (2014), which showed that adding an excess of calcium cations to a K_2SO_4 solution favored the formation of gypsum while reducing syngenite and görgeyite content in the solid phase. Syngenite, which contains more bound water than görgeyite, undergoes a crystalline transition to görgeyite, arcanite, and water at 227 °C (Kloprogge et al., 2004). Thus, there is a greater likelihood that syngenite was the predominant crystalline form produced in this study since the urine temperature remained below 70 °C.

In addition to potassium, both ammonium (Fig. 5b) and chloride (Fig. 5e) showed a tendency to partition into the solid phase at urine CFs >20. It is probable that ammonium and potassium cations crystallized with chloride anions to form either salammoniac or sylvite. Indeed, Yu et al. (2012) observed that in a KCl - NH_4Cl - H_2O system at 25 °C, the crystallization fields of the two solid solutions [(K, NH_4)Cl] and [(NH_4, K)Cl] occupied almost the entire phase region. This indicates that potassium and ammonium readily form a solid solution with chloride anions rather than crystallizing as single salts. This provides an explanation for the similar partitioning behavior of ammonium and potassium that was observed in this study and suggests that separating these ions by a stepwise dehydration-crystallization process would be difficult.

The drop in orthophosphate content in the liquid phase at urine CFs above 30 (Fig. 5c) is likely due to its crystallization with potassium to form biphosphammite. According to Jiang et al. (2017), biphosphammite ($NH_4H_2PO_4$) is one of the major crystals that form in acidified urine after evaporation, noting that its saturation solubility at 25 °C is the lowest among all the crystals they observed. In their study, urine was hydrolyzed, resulting in a relatively high ammonium concentration that led to the formation of biphosphammite as a combination of phosphate and ammonia ($NH_4H_2PO_4$). Contrastingly, in this study the acidified and unhydrolyzed urine had a potassium concentration ten times higher than that of ammonium. Consequently, the biphosphammite that formed was likely a combination of potassium and orthophosphate (KH_2PO_4). Nonetheless, because the ionic radii of potassium and ammonium are similar, their crystal structures with phosphate are identical (Frost et al., 2011). Therefore, the solubility of biphosphammite in the form of KH_2PO_4 is deduced to be similarly low as that of $NH_4H_2PO_4$ at 25 °C. The biphosphammite (KH_2PO_4) formed in this study is considered a major component of the crystalline solids.

5. Conclusion

This study demonstrates that stepwise evaporation-crystallization of acidified human urine is an effective method for producing multinutrient fertilizers with different nutrient profiles. By controlling dehydration conditions, it is possible to achieve high concentration factors (CF 30 at 20 °C and CF 43 at 70 °C) without nutrient losses, thereby disproving concerns regarding nitrogen loss during urine processing via acidification and dehydration. Monitoring water activity in urine proved to be a reliable approach for managing the drying process. Notably, a critical water activity threshold of 0.3 at CF 43 was identified, beyond which further dehydration was constrained by tightly bound water, and thus, could be targeted in practical drying applications. Moreover, this study identified the crystallization sequence of urine constituents under varying evaporation conditions. Initially, calcium sulfate crystallizes as gypsum when urine is concentrated to CF between 10 and 20. As dehydration progresses to CF 30, potassium and sulfate crystallize with previously formed gypsum as syngenite, while potassium/ammonium chloride and biphosphammite crystallize at higher CFs. Notably, over 80 % of urea, ammonium, and orthophosphate remained in the liquid phase up to CF 30, while sulfate and potassium predominantly partitioned into the solid phase. This selective crystallization behavior provides a strategy for tailoring urine-derived fertilizers to specific environmental needs, such as minimizing salt content for sensitive or arid soils, thereby mitigating risks such as soil salinization.

CRediT authorship contribution statement

Ya Gao: Writing – review & editing, Writing – original draft, Visualization, Software, Methodology, Investigation, Formal analysis, Data curation, Conceptualization. **Björn Vinnerås:** Writing – review & editing, Supervision, Resources, Methodology, Funding acquisition, Conceptualization. **Prithvi Simha:** Writing – review & editing, Supervision, Resources, Methodology, Investigation, Funding acquisition, Formal analysis, Conceptualization.

Declaration of competing interest

Prithvi Simha and Björn Vinnerås are co-owners of Sanitation360 AB, a university spin-off commercialising various technologies for recycling human urine. The authors declare that the work reported in this study was not influenced by their involvement in this company.

Acknowledgements

This study was supported by funding from the European Union's Horizon Europe Research and Innovation Programme for the project “P2Green: Closing the gap between fork and farm for circular nutrient flows” (Grant number 101081883). We acknowledge colleagues at SLU who donated urine and supported our research. We thank Foon Yin Lai for assistance with centrifugation, and Kretsloppsteknik Group for discussion and feedback during the presentation of the work.

Appendix A. Supplementary data

Supplementary data to this article can be found online at https://doi.org/10.1016/j.scitotenv.2025.178709.

Data availability

Data will be made available on request.

References

Aliahmad, A., Harder, R., Simha, P., Vinnerås, B., McConville, J., 2022. Knowledge evolution within human urine recycling technological innovation system (TIS): focus on technologies for recovering plant-essential nutrients. J. Clean. Prod. 379, 134786. https://doi.org/10.1016/j.jclepro.2022.134786.

Blandamer, M.J., Engberts, J., Gleeson, P.T., Reis, J.C.R., 2005. Activity of water in aqueous systems; A frequently neglected property. Chem. Soc. Rev. 34 (5), 440–458. https://doi.org/10.1039/b400473f.

Chowdhury, M.A., de Neergaard, A., Jensen, L.S., 2014. Prediction of changes in important physical parameters during composting of separated animal slurry solid fractions. Environ. Technol. 35 (2), 220–231. https://doi.org/10.1080/09593330.2013.824008.

Freyer, D., Voigt, W., 2003. Crystallization and phase stability of $CaSO_4$ and $CaSO_4$ – based salts. Monatshefte Fur Chemie 134 (5), 693–719. https://doi.org/10.1007/s00706-003-0590-3.

Frost, R. L., Xi, Y. F., & Palmer, S. J. (2011). Are the 'cave' minerals archerite (K,NH_4) H_2PO_4 and biphosphammite (K,NH_4)H_2PO_4 identical? A molecular structural study. J. Mol. Struct., 1001(1–3), 49–55. doi:https://doi.org/10.1016/j.molstruc.2011.06.015.

Getahun, S., Septien, S., Mata, J., Somorin, T., Mabbett, I., Buckley, C., 2020. Drying characteristics of faecal sludge from different on-site sanitation facilities. J. Environ. Manag. *261*, Article 110267. https://doi.org/10.1016/j.jenvman.2020.110267.

Guizani, M., Fujii, T., Hijikata, N., Funamizu, N., 2016. Salt removal from soil during rainy season of semi-arid climate following an assumed salt accumulation from previous cultivations fertilized with urine. *Euro-Mediterranean journal for environmental.* Integration 1(1), Article 10. https://doi.org/10.1007/s41207-016-0010-9.

Harder, R., Wielemaker, R., Larsen, T.A., Zeeman, G., Öberg, G., 2019. Recycling nutrients contained in human excreta to agriculture: pathways, processes, and products. Crit. Rev. Environ. Sci. Technol. 49 (8), 695–743.

Hasan, H.A.H., 2000. Ureolytic microorganisms and soil fertility: A review. Commun. Soil Sci. Plant Anal. 31 (15–16), 2565–2589. https://doi.org/10.1080/00103620009370609.

Hellström, D., Johansson, E., Grennberg, K., 1999. Storage of human urine: acidification as a method to inhibit decomposition of urea. Ecol. Eng. 12 (3), 253–269. https://doi.org/10.1016/S0925-8574(98)00074-3.

Hostmark, O., Teigland, S., 2009. Role of water activity of liquid in controlling evaporation rate of low-viscosity liquids. Dry. Technol. 27 (10), 1152–1155. Article Pii 915830884. https://doi.org/10.1080/07373930903221747.

Jain, M., Raghavan, V., 2024. Global publication trend in the field of resource recovery from wastewater: A bibliometric analysis. Water Practice and Technology. https://doi.org/10.2166/wpt.2024.164.

Jiang, S.Q., Wang, X.C., Yang, S.J., Shi, H.L., 2017. Effect of initial pH and pH-adjusted acid on nutrient recovery from hydrolysis urine by combining acidification with evaporation-crystallization. Environ. Sci. Pollut. Res. 24 (4), 3872–3881. https://doi.org/10.1007/s11356-016-8052-8.

Jönsson, H., Baky, A., Jeppsson, U., högskola, C. t., 2005. Composition of Urine, Faeces, Greywater and Biowaste for Utilisation in the URWARE Model. Urban Water,. Chalmers University of Technology.

Jurisová, J., Danielik, V., Fellner, P., Lencsés, M., Králik, M., 2014. Phase diagram of the system $CaSO_4$-K_2SO_4-KNO_3-ca$(NO_3)_2$-H_2O. Acta Chim. Slov. 7 (1), 20–24. https://doi.org/10.2478/acs-2014-0004.

Kirchmann, H., Pettersson, S., 1995. Human urine - chemical-composition and fertilizer use efficiency. Fertilizer Research 40 (2), 149–154. https://doi.org/10.1007/bf00750100.

Kloprogge, J.T., Ding, Z., Martens, W.N., Schuiling, R.D., Duong, L.V., Frost, R.L., 2004. Thermal decomposition of syngenite, $K_2Ca(SO_4)_2 \cdot H_2O$. Thermochim. Acta 417 (1), 143–155. https://doi.org/10.1016/j.tca.2003.12.001.

Litalien, A., Zeeb, B., 2020. Curing the earth: A review of anthropogenic soil salinization and plant-based strategies for sustainable mitigation. Sci. Total Environ. 698, Article 134235. https://doi.org/10.1016/j.scitotenv.2019.134235.

Martin, T.M.P., Esculier, F., Levavasseur, F., Houot, S., 2022. Human urine-based fertilizers: A review. Crit. Rev. Environ. Sci. Technol. 52 (6), 890–936. https://doi.org/10.1080/10643389.2020.1838214.

Maurer, M., Pronk, W., Larsen, T., 2006. Treatment processes for source-separated urine. Water Res. 40 (17), 3151–3166.

Medeiros, D.L., Queiroz, L.M., Cohim, E., Almeida-Neto, J.A., d., & Kiperstok, A., 2020. Human urine fertiliser in the Brazilian semi-arid: environmental assessment and water-energy-nutrient nexus. Sci. Total Environ. 713, 136145. https://doi.org/10.1016/j.scitotenv.2019.136145.

Mobley, H.L.T., Hausinger, R.P., 1989. Microbial ureases - significance, regulation. AND MOLECULAR CHARACTERIZATION. Microbiological Reviews 53 (1), 85–108. https://doi.org/10.1128/mmbr.53.1.85-108.1989.

Nielsen, O.F., Bilde, M., Frosch, M., 2012. Water activity. *Spectroscopy-an.* Int. J. 27 (5–6), 565–569. https://doi.org/10.1155/2012/414635.

Oki, K., Washio, K., Matsui, D., Kato, S., Hirata, Y., Morikawa, M., 2010. The role of urease activity on biofilm formation by Staphylococcus sp. T-02 isolated from the toilet bowl. Biosci. Biotechnol. Biochem. 74 (3), 583–589. https://doi.org/10.1271/bbb.90796.

Otterpohl, R., Braun, U., Oldenburg, M., 2002. Innovative technologies for decentralised wastewater management in urban and peri-urban areas. Berichte-Wassergute Und Abfallwirtschaft Technische Universitat Munchen Berichtsheft 173, 109–126.

Parambil, J. V., & Heng, J. Y. Y. (2017). Seeding in crystallisation. In K. J. Roberts, R. Docherty, & R. Tamura (Eds.), *engineering crystallography: from molecule to crystal to functional form* (pp. 235-245). doi:https://doi.org/10.1007/978-94-024-1117-1_13.

Peces, M., Astals, S., Mata-Alvarez, J., 2014. Assessing total and volatile solids in municipal solid waste samples. Environ. Technol. 35 (24), 3041–3046. https://doi.org/10.1080/09593330.2014.929182.

Putnam, D.F., 1971. Composition and Concentrative Properties of Human Urine.

Shaw, W.H.R., 1954. The inhibition of urease by various metal ions. J. Am. Chem. Soc. 76 (8), 2160–2163. https://doi.org/10.1021/ja01637a034.

Shokri-Kuehni, S.M.S., Vetter, T., Webb, C., Shokri, N., 2017. New insights into saline water evaporation from porous media: complex interaction between evaporation rates, precipitation, and surface temperature. Geophys. Res. Lett. 44 (11), 5504–5510. https://doi.org/10.1002/2017gl073337.

Simha, P., Deb, C.K., Randall, D.G., Vinnerås, B., 2022. Thermodynamics and kinetics of pH-dependent dissolution of sparingly soluble alkaline earth hydroxides in source-separated human urine collected in decentralised sanitation systems. *Frontiers in environmental.* Science 10, Article 889119. https://doi.org/10.3389/fenvs.2022.889119.

Simha, P., Lalander, C., Nordin, A., Vinnerås, B., 2020. Alkaline dehydration of source -separated fresh human urine: preliminary insights into using different dehydration temperature and media. Sci. Total Environ. 733, Article 139313. https://doi.org/10.1016/j.scitotenv.2020.139313.

Simha, P., Vasiljev, A., Randall, D.G., Vinnerås, B., 2023. Factors influencing the recovery of organic nitrogen from fresh human urine dosed with organic/inorganic acids and concentrated by evaporation in ambient conditions. Sci. Total Environ. 879, Article 163053. https://doi.org/10.1016/j.scitotenv.2023.163053.

Todd, M.J., Hausinger, R.P., 1989. Competitive inhibitors of KLEBSIELLA-AEROGENES urease - mechanisms of interaction with the nickel active-site. J. Biol. Chem. 264 (27), 15835–15842.

Trimmer, J.T., Guest, J.S., 2018. Recirculation of human-derived nutrients from cities to agriculture across six continents. Nature Sustainability 1 (8), 427–435. https://doi.org/10.1038/s41893-018-0118-9.

Udert, K.M., Larsen, T.A., Biebow, M., Gujer, W., 2003. Urea hydrolysis and precipitation dynamics in a urine-collecting system. Water Res. 37 (11), 2571–2582. https://doi.org/10.1016/S0043-1354(03)00065-4.

Vinnerås, B., Palmquist, H., Balmér, P., Jönsson, H., 2006. The characteristics of household wastewater and biodegradable solid waste—A proposal for new Swedish design values. Urban Water J. 3 (1), 3–11. https://doi.org/10.1080/15730620600578629.

Voigt, W., 2001. Solubility equilibria in multicomponent oceanic salt systems from $t = 0$ to 200 °C. Model parameterization and databases. 73 (5), 831–844. https://doi.org/10.1351/pac200173050831.

Yu, X. D., Zeng, Y., & Zhang, Z. X. (2012). Solid–Liquid Metastable Phase Equilibria in the Ternary Systems $KCl + NH_4Cl + H_2O$ and $NH_4Cl + MgCl_2 + H_2O$ at 298.15 K. J. Chem. Eng. Data, 57(6), 1759–1765. doi:https://doi.org/10.1021/je300124u.